Progress In Electromagnetics Research, PIER 74, 319–340, 2007

DESIGN EQUATIONS OF TWO-DIMENSIONAL DIELECTRIC PHOTONIC BAND GAP STRUCTURES

M. A. El-Dahshory

Telecom Egypt, Egypt

A. M. Attiya

Electronics Research Institute, Egypt

E. A. Hashish

Department of Electronics and Communications
Faculty of Engineering
Cairo University
Egypt

Abstract—This paper presents simple formulas for designing different configurations of two-dimensional photonic band gap (PBG) structures. These formulas are obtained by interpolating full wave analysis based on the plane wave expansion method. The design parameters of these formulas include the physical dimensions of the unit cell and the electrical properties of both host and inclusion in the structure. These formulas represent an efficient and fast method to obtain the band gap and the center frequency of different PBG structures.

1. INTRODUCTION

The wave propagation in periodic structure has attracted many researchers to investigate the properties of these structures over the past ten years [1]. Photonic band gap structures have frequency stop bands over which the propagation of electromagnetic waves are forbidden in certain or all directions. The band gap frequency in such periodic structure depends on many factors such as host and inclusion dielectric constants, lattice type, filling fraction, periodicity, and angle of incidence.

PBG structures were initially applied to optical applications like high-quality optical mirrors and resonators [2–6]. By scaling optical PBG structures, electromagnetic crystals could be realized to be used in the microwave range. Recently, many potential applications have been introduced for 1-D, 2-D, and 3-D electromagnetic band gap structures [7–12]. The present paper is mainly focused on 2-D dielectric PBG structures. Figure 1 shows schematic diagrams for the cross sections of general 2-D square and triangular PBG structures.

Analysis of photonic band gap structures has been discussed by different techniques such as method of moment [13], transfer matrix

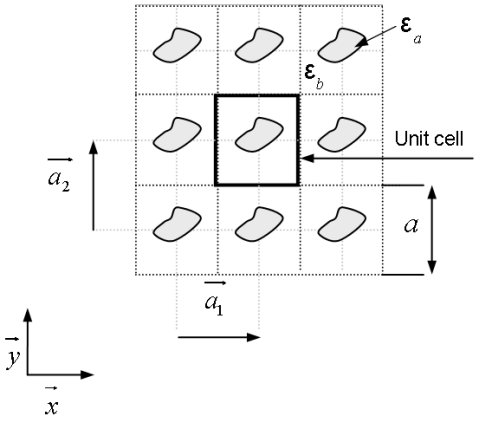

(a) Square lattice. $\vec{a}_1 = a\hat{x},\ \vec{a}_2 = a\hat{y}$.

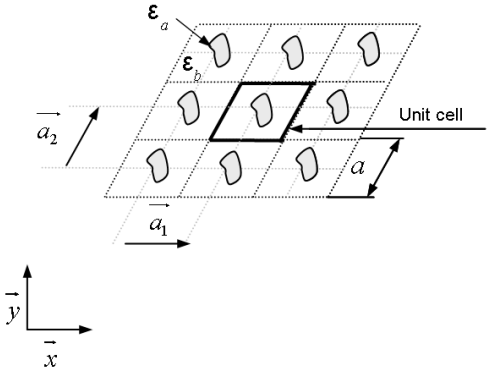

(b) Triangular lattice. $\vec{a}_1 = a\hat{x},\ \vec{a}_2 = a(0.5\hat{x} + 0.5\sqrt{3}\hat{y})$.

Figure 1. Geometry of a 2-D PBG structure on (a) square lattice, (b) triangular lattice. ($\vec{a}_1$ and $\vec{a}_2$) are the basis vectors. (ε_a and ε_b) are the dielectric constants of both the inclusion and the host respectively.

method [14], finite difference time domain [15], finite element method [16] and plane wave expansion method [17]. Each method has its own advantages and disadvantages that make it more appropriate to simulate specific problems related to PBG structure. However, a common disadvantage in all these method is the large computational requirements to calculate the band gap diagram. The motivation of this paper is to introduce simple design equations based on interpolating the full wave results of different PBG structures. The analysis of the present paper is based on the plane wave method and its also verified by using FDTD.

The plane wave method has been found to be a simple and efficient method to obtain the dispersion relation of different PBG configurations [17]. The following section presents a brief description of this method for different cases including rectangular and triangular lattice grids. Then this method is applied on different configurations of PBG structures to obtain their corresponding band gap diagrams. These different configurations include different shapes of implanted dielectric rods, different dielectric constants and different polarizations. By interpolating the corresponding results, we could obtain design equations for the width of the band gaps and the corresponding center frequencies for these different configurations. These design equations can be used as a fast designing tool to design 2-D PBG structures. A design example is presented to show how one can use these equations to design a 2-D PBG structure of specific rod type, specific center frequency and bandwidth.

2. THEORY AND ANALYSIS

This section presents a brief description of plane wave method to obtain the dispersion diagram of two-dimensional PGB structures. More details can also be found in previously published papers [17, 19]. In this method, the total field of a periodic structure is represented as a superposition of infinite discrete spectral components. Each spectral component represents either a propagating or an evanescent plane wave. These discrete components have the same periodicity of the periodic boundary condition. Most of PBG structures are based on non-magnetic material. Thus, it is preferred to formulate the problem in terms of the magnetic field to avoid the discontinuity of the normal component of the electric field at the interface between the host and the inclusion. Such magnetic field in an infinite 2-D periodic structure can be represented as

$$\boldsymbol{H}(r) = e^{j\boldsymbol{k}\cdot\boldsymbol{r}} \sum_{\boldsymbol{G}} \sum_{j=1,2} \hat{e}_j H_{j,\boldsymbol{k}}(\boldsymbol{G}) e^{j\boldsymbol{G}\cdot\boldsymbol{r}} \tag{1}$$

where $\boldsymbol{r}$ is the vector in the lattice plane, $\boldsymbol{k}$ is the lattice vector, $\boldsymbol{G}$ is the reciprocal lattice vector, $\hat{e}_j$ is the unit vector parallel to the direction of the magnetic field where $j = 1$ corresponds to TM_z wave and $j = 2$ corresponds to TE_z wave, and $H(\boldsymbol{G})$ is the Fourier expansion of the magnetic field.

The wave equation of the magnetic field in a spatial varying medium is

$$\nabla \times \frac{1}{\varepsilon(\boldsymbol{r})} \nabla \times \boldsymbol{H}(\boldsymbol{r}) = \frac{\omega^2}{c^2} \boldsymbol{H}(\boldsymbol{r}) \tag{2}$$

By applying the spectral representation of Eq. (1) into the above magnetic field wave equation and taking into consideration the directions of the TM_z and the TE_z components of the magnetic field, one can obtain the following eigenvalue problems for both TM and TE waves [17]

$$\sum_{\boldsymbol{G}'} |\boldsymbol{k} + \boldsymbol{G}||\boldsymbol{k} + \boldsymbol{G}'| \varepsilon^{-1}(\boldsymbol{G} - \boldsymbol{G}') H_{1,\boldsymbol{k}}(\boldsymbol{G}') = \frac{\omega^2}{c^2} H_{1,\boldsymbol{k}}(\boldsymbol{G}) \tag{3a}$$

$$\sum_{\boldsymbol{G}'} (\boldsymbol{k} + \boldsymbol{G}) \cdot (\boldsymbol{k} + \boldsymbol{G}') \varepsilon^{-1}(\boldsymbol{G} - \boldsymbol{G}') H_{2,\boldsymbol{k}}(\boldsymbol{G}') = \frac{\omega^2}{c^2} H_{2,\boldsymbol{k}}(\boldsymbol{G}) \tag{3b}$$

where $\varepsilon(\boldsymbol{G})$ is the Fourier transformation of the relative dielectric constant $\varepsilon(\boldsymbol{r})$ given by:

$$\varepsilon(\boldsymbol{G}) = \frac{1}{A} \int_A \varepsilon(\boldsymbol{r}) e^{-j\boldsymbol{G}\cdot\boldsymbol{r}} d\boldsymbol{r} \tag{4}$$

where $\varepsilon(\boldsymbol{r})$ is the dielectric constant as a function of the position inside the lattice, $\boldsymbol{r}$ is the coordinate in a plane perpendicular to the rods, and A is the area of the lattice unit cell. Equation (4) can be simplified as:

$$\varepsilon(\boldsymbol{G}) = \begin{cases} \beta\varepsilon_a + (1-\beta)\varepsilon_b & \text{for } \boldsymbol{G} = 0 \\ (\varepsilon_a - \varepsilon_b) S(\boldsymbol{G}) & \text{for } \boldsymbol{G} \neq 0 \end{cases} \tag{5}$$

where β is the filling fraction, defined as the area of the rod to the area of the unit cell and $S(\boldsymbol{G})$ is the structure factor that depends on the geometry of both the rod and the lattice as follows:

$$S(\boldsymbol{G}) = \frac{1}{A} \int_{\text{inclusion}} e^{-j\boldsymbol{G}\cdot\boldsymbol{r}} d\boldsymbol{r} \tag{6}$$

In the present analysis, $S(\boldsymbol{G})$ is calculated for different structures for both rectangular and triangular lattice as shown in Fig. 1. To calculate

the band gap, the $\boldsymbol{k}$ vector is calculated around the boundaries of the irreducible Brillouin zone [18] as shown in Fig. 2. The remaining points inside the irreducible Brillouin zone can be obtained by interpolating the values at its boundaries.

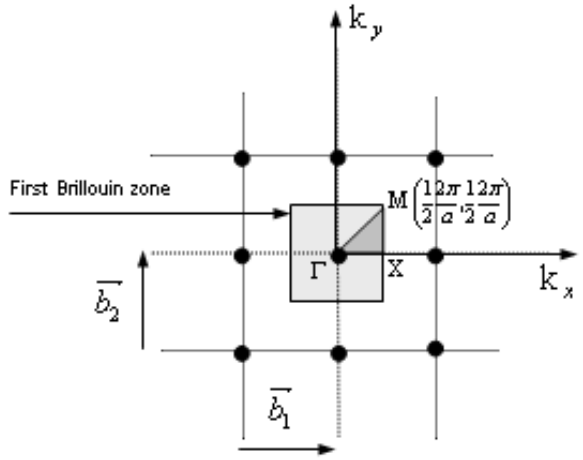

(a) Reciprocal space of square lattice. $\vec{b}_1 = \frac{2\pi}{a}$, $\vec{b}_2 = \frac{2\pi}{a}$.

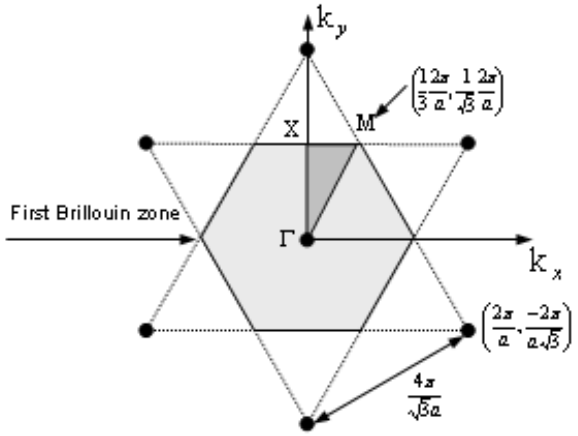

(b) Reciprocal space of triangular lattice. $\vec{b}_1 = \frac{2\pi}{a}\left(\hat{x} - \frac{1}{\sqrt{3}}\hat{y}\right)$, and $\vec{b}_2 = \frac{2\pi}{a}\frac{2}{\sqrt{3}}\hat{y}$.

Figure 2. The reciprocal lattices of the PBG structures. The reciprocal lattice bases are ($\vec{b}_1$ and $\vec{b}_2$). The light shading area is the first Brillouin zone; the dark shading area is the irreducible Brillouin zone and the dark points are the reciprocal lattice points.

3. DESIGN EQUATIONS OF TWO-DIMENSIONAL PBG

In this section rectangular and triangular lattice PBG structures of different rod shapes are investigated for both TM and TE polarization by using PWM. Then the results of these different configurations are interpolated to obtain design equations for these configurations. The present analysis is based on truncating the infinite matrix of the corresponding eigenvalue problem in Eq. (3) to $N \times N$ where N is chosen to be eleven. It is found that such number of expansion functions is enough for a good accuracy and it is also suitable for simulation time. The band gap width considered here is basically the band gap between the first two modes of the structure if nothing else is mentioned.

Figure 3 shows the calculated relative bandwidth of the first band gap $\Delta\omega/\omega_0$ as a function of the filling fraction β for different index ratios $\alpha = \varepsilon_a/\varepsilon_b$. The negative value of $\Delta\omega/\omega_0$ indicates that there is an overlap region between the dispersion curves of the first and the second modes. This means that the real band gap would correspond to the positive values of $\Delta\omega/\omega_0$ only. The results shown in Fig. 3 represent both square and triangular lattices of circular rods. The lattice constant in both cases is $a = 12\,\text{mm}$. For the case where the index ratio is greater than unity, $\alpha > 1$, the dominant band gap is found to be of TM polarization as shown in Figs. 3(a) and (b). In this case, it can be noted that increasing the index ratio causes the peak of the relative bandwidth to take place at a smaller value of the filling fraction. On the other hand, for the case of , the dominant band gap is found to be of TE polarization as shown in Figs. 3(c) and (d). In this case, decreasing the index ratio causes the peak of the relative bandwidth to take place at a larger value of the filling fraction. Figure 3(d) also shows that the relative bandwidth has a considerable values in triangular lattice case for different values of $\alpha \leq 1/2$ while in square lattice case the relative bandwidth values exist for $\alpha \leq 1/6$, Fig. 3(c).

The value of $\beta_{\max}$ would be defined here as the optimum value of filling fraction β where the maximum relative bandwidth occurs for certain value of the index ratio α. This value represents an important designing factor to obtain the maximum available bandwidth of a certain PBG structure.

By getting the peaks of Fig. 3 for different values of α and interpolating the obtained results, one can obtain the designing equation

$$\beta_{\max}(\alpha) = \sum_{n=0}^{N} a_n \alpha^n \tag{7}$$

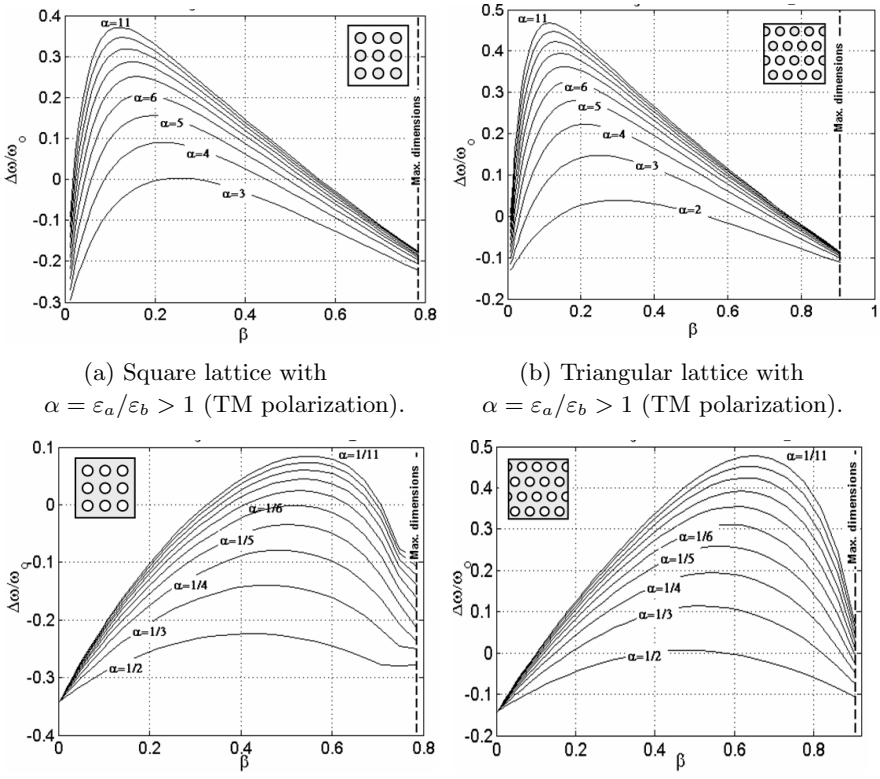

(a) Square lattice with $\alpha = \varepsilon_a/\varepsilon_b > 1$ (TM polarization).

(b) Triangular lattice with $\alpha = \varepsilon_a/\varepsilon_b > 1$ (TM polarization).

(c) Square lattice with $\alpha = \varepsilon_a/\varepsilon_b < 1$ (TE polarization).

(d) Triangular lattice with $\alpha = \varepsilon_a/\varepsilon_b < 1$ (TE polarization).

Figure 3. The relative band width $\Delta\omega/\omega_0$ versus filling fraction β for different index ratio $\alpha = \varepsilon_a/\varepsilon_b$ of circular rods. The lattice constant $a = 12\,\text{mm}$. The dotted line is the maximum limit of the filling fraction.

For the case of a square lattice of circular rods, the value of $\beta_{\max}$ as a function of the index ratio for $\alpha > 1$ Fig. 4(a) is found to be:

$$\begin{aligned}\beta_{\max}(\alpha) \;=\; & -4.141\times10^{-6}\alpha^5 + 1.6899\times10^{-4}\alpha^4 - 2.7977\times10^{-3}\alpha^3 \\ & +2.4554\times10^{-2}\alpha^2 - 0.12827\alpha + 0.47809 \end{aligned} \tag{8a}$$

While for $\alpha < 1$ Fig. 4(c):

$$\beta_{\max}(\alpha) = 0.34147\alpha^2 - 0.53021\alpha + 0.59739 \tag{8b}$$

Figures 4(a) and (c) show a comparison between the calculated $\beta_{\max}$ and the corresponding design equation for the case of a square lattice

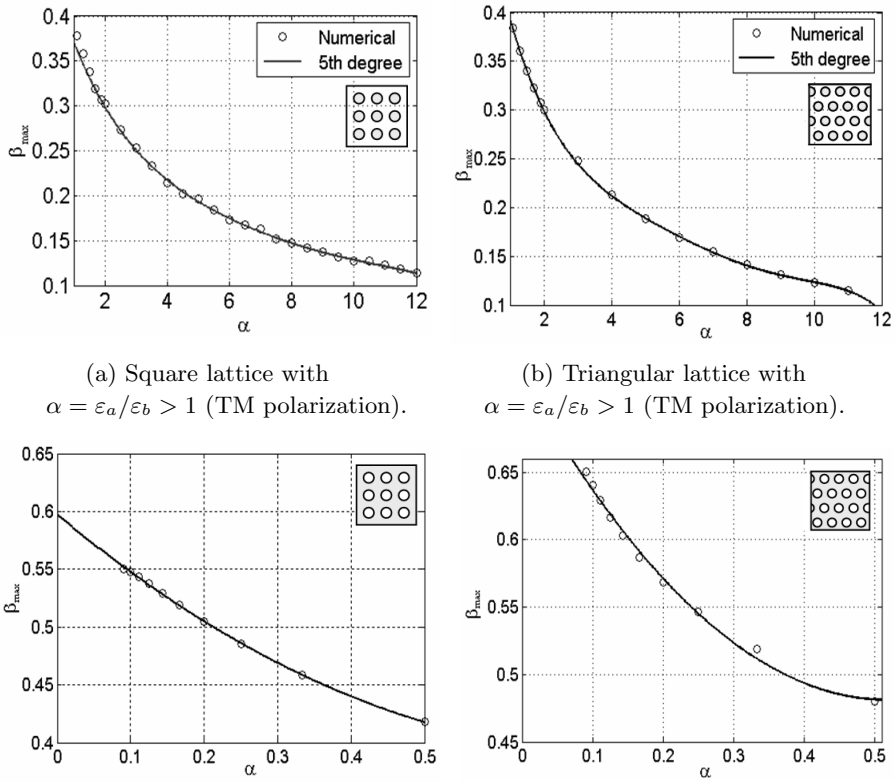

(a) Square lattice with $\alpha = \varepsilon_a/\varepsilon_b > 1$ (TM polarization).

(b) Triangular lattice with $\alpha = \varepsilon_a/\varepsilon_b > 1$ (TM polarization).

(c) Square lattice with $\alpha = \varepsilon_a/\varepsilon_b < 1$ (TE polarization).

(d) Triangular lattice with $\alpha = \varepsilon_a/\varepsilon_b < 1$ (TE polarization).

Figure 4. $\beta_{\max}$ versus α for circular rods.

of circular rods. Similarly, Figures 4(b) and (d) show the same comparison for the case of the triangular lattice of circular rods. It can be noticed the good agreement between the actual results and the corresponding design equations.

These peaks of the relative maximum bandwidth can also be interpolated as a function of $\beta_{\max}$ as follows

$$\max(\Delta\omega/\omega_0) = \sum_{m=0}^{M} b_m(\beta_{\max}(\alpha))^m \tag{9}$$

This function represents another important designing equation where it is usually required to increase the relative bandwidth. For the case of a square lattice of circular rods, the maximum relative bandwidth is given by

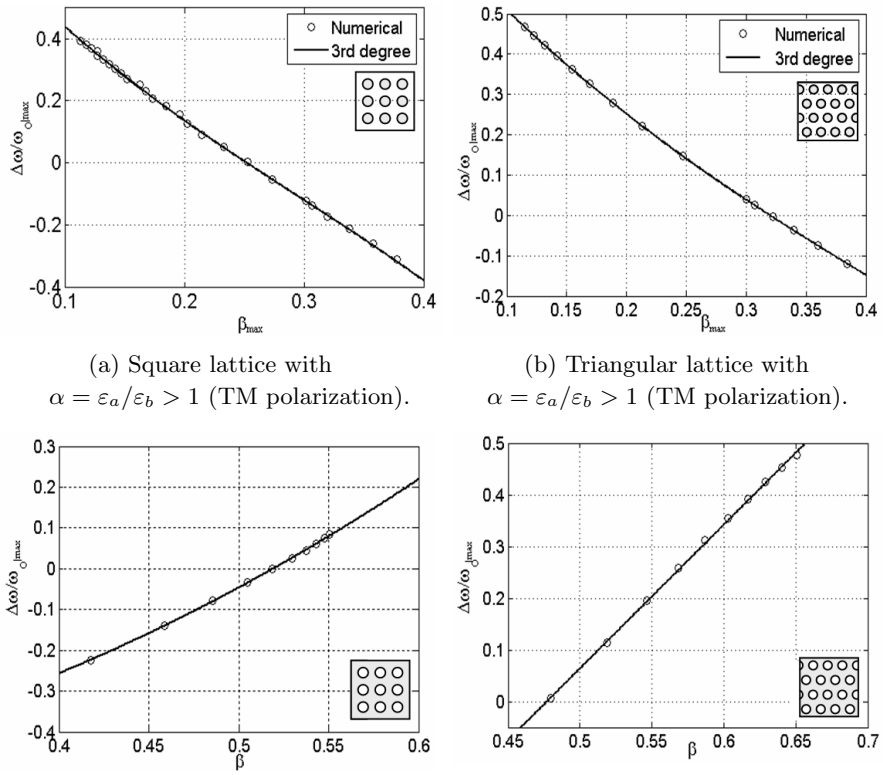

(a) Square lattice with $\alpha = \varepsilon_a/\varepsilon_b > 1$ (TM polarization).

(b) Triangular lattice with $\alpha = \varepsilon_a/\varepsilon_b > 1$ (TM polarization).

(c) Square lattice with $\alpha = \varepsilon_a/\varepsilon_b < 1$ (TE polarization).

(d) Triangular lattice with $\alpha = \varepsilon_a/\varepsilon_b < 1$ (TE polarization).

Figure 5. $\Delta\omega/\omega_0|_{\max}$ versus $\beta_{\max}$ for circular rods.

for $\alpha > 1$, Fig. 5(a)

$$\max(\Delta\omega/\omega_0) = -8.3658\beta_{\max}^3 + 7.3676\beta_{\max}^2 - 4.6609\beta_{\max} + 0.84218 \tag{10a}$$

While for $\alpha < 1$, Fig. 5(c)

$$\max(\Delta\omega/\omega_0) = 2.7544\beta_{\max}^2 - 0.3744\beta_{\max} - 0.54748 \tag{10b}$$

Figure 5 shows a comparison between the calculated maximum relative bandwidth and the corresponding value obtained by the design equations for both square and triangular lattices of circular rods.

The remaining designing parameter that should be considered is the center frequency of the maximum relative bandwidth; f_0; at $\beta = \beta_{\max}$ which is a function of the lattice constant, the index

ratio, the filling ratio and the dielectric constant of the host. It is found that, direct interpolation of such central frequency is usually weakly convergent. Thus, it is preferred to interpolate the reciprocal normalized central frequency defined as $1/(f_0\sqrt{\varepsilon_b}a)$. For $\alpha > 1$, such reciprocal normalized central frequency can be approximated as

$$1/\left(f_0\sqrt{\varepsilon_b}a\right) = \sum_{v=0}^{N} c_v a^v \tag{11a}$$

On the other hand, for PBG with $\alpha < 1$, the reciprocal normalized central frequency can be approximated as

$$1/\left(f_0\sqrt{\varepsilon_b}a\right) = \sum_{v=0}^{N} c_v a^{-v} \tag{11b}$$

For the case of the square lattice of circular dielectric rods, the central frequency is given by for $\alpha > 1$, Fig. 6(a),

$$f_0(a,\alpha) = \frac{1/\sqrt{\varepsilon_b}a}{\left[\begin{array}{c} 1.5385\times10^{-7}\alpha^5 - 4.9417\times10^{-6}\alpha^4 + 6.3124\times10^{-5}\alpha^3 \\ -4.2991\times10^{-4}\alpha^2 + 1.8655\times10^{-3}\alpha + 4.2527\times10^{-3} \end{array}\right]} \tag{12a}$$

while for $\alpha < 1$ Fig. 6(c)

$$f_0(a,\alpha) = \frac{1/\sqrt{\varepsilon_a}a}{\left[\begin{array}{c} 3.0923\times10^{-6}\alpha^{-3} - 7.9818\times10^{-5}\alpha^{-2} \\ +1.0737\times10^{-3}\alpha^{-1} + 4.94\times10^{-3} \end{array}\right]} \tag{12b}$$

where f is in (GHz) and a is in (mm). Figure 6 shows a comparison between the calculated reciprocal normalized central frequency and the corresponding interpolation as a function of index ratio for both square and triangular lattices of circular rods.

The previous analyses are applied on different configurations of PBG structures as shown in Figures 7 and 8 [19]. These configurations include square and triangular lattice in both cases TE and TM polarizations for $\alpha > 1$ and for $\alpha < 1$. The design equations of these structures are summarized in the Appendix. From the analysis of these PBG configurations in square and triangular lattice, it is found that each configuration has special band gap properties. These properties could be classified according to the existence of a complete band gap, or the existence of a band gap at higher order modes as shown in Appendix. It should also be noted that this analysis is valid for any frequency range due to the scalability of the PBG structures.

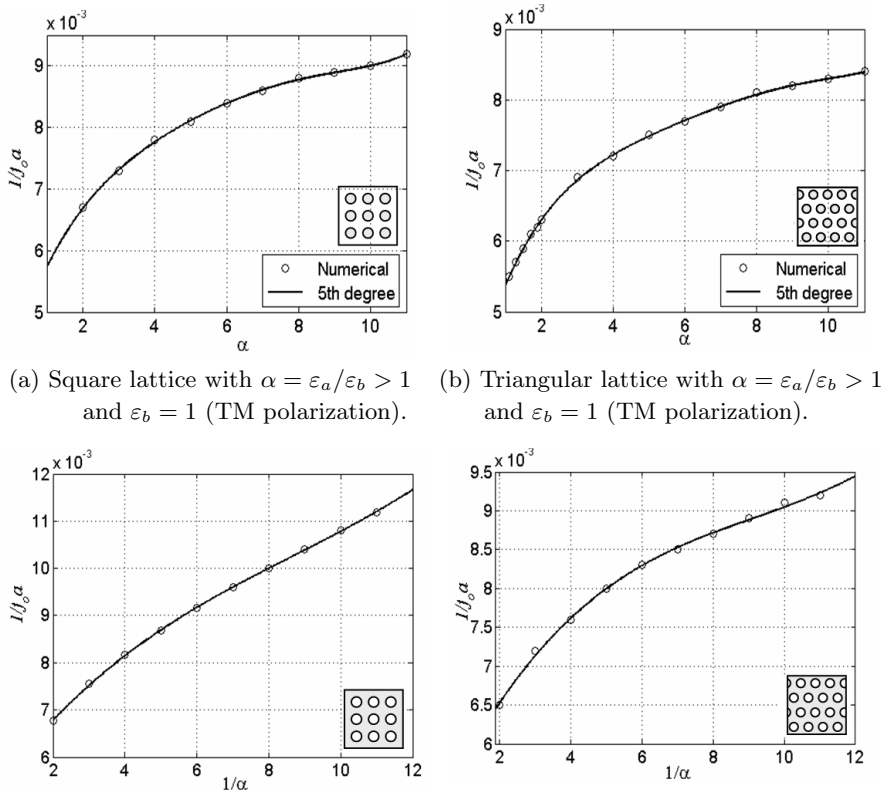

(a) Square lattice with $\alpha = \varepsilon_a/\varepsilon_b > 1$ and $\varepsilon_b = 1$ (TM polarization).

(b) Triangular lattice with $\alpha = \varepsilon_a/\varepsilon_b > 1$ and $\varepsilon_b = 1$ (TM polarization).

(c) Square lattice with $\alpha = \varepsilon_a/\varepsilon_b < 1$ and $\varepsilon_a = 1$ (TE polarization).

(d) Triangular lattice with $\alpha = \varepsilon_a/\varepsilon_b < 1$ and $\varepsilon_a = 1$ (TE polarization).

Figure 6. $1/f_0 a$ versus α, the filling fraction is set at maximum value for different values of α. f is in (GHz) and a is in (mm).

4. DESIGN EXAMPLE OF A PBG STRUCTURE BY USING THE DEVELOPED EQUATIONS

Assuming that it is required to design a PBG structure of square lattice with circular dielectric rods in microwave range where the center frequency of its band gap is $f_0 = 6\,\text{GHz}$ and the required band gap is $\Delta f = 2\,\text{GHz}$ for TM polarization. Thus, the required steps to design a PBG structure with these required specifications are as follows:

(a) Using the maximum relative bandwidth equation (9a)

For $\Delta f/f_0 = 1/3$, $\beta_{\max}$ is found to be as shown in Fig. 9(a)

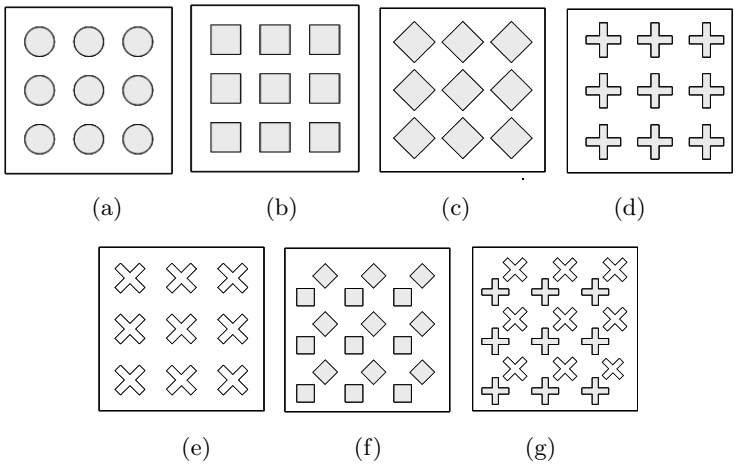

Figure 7. Rod shapes and configurations considered in square lattice. (a) square-circle (SC). (b) square-square (SS). (c) square-rotated square (SRS). (d) square-cross (SCR). (e) square-rotated cross (SRCR). (f) square-mixed square (SMS). (g) square-mixed cross (SMCR).

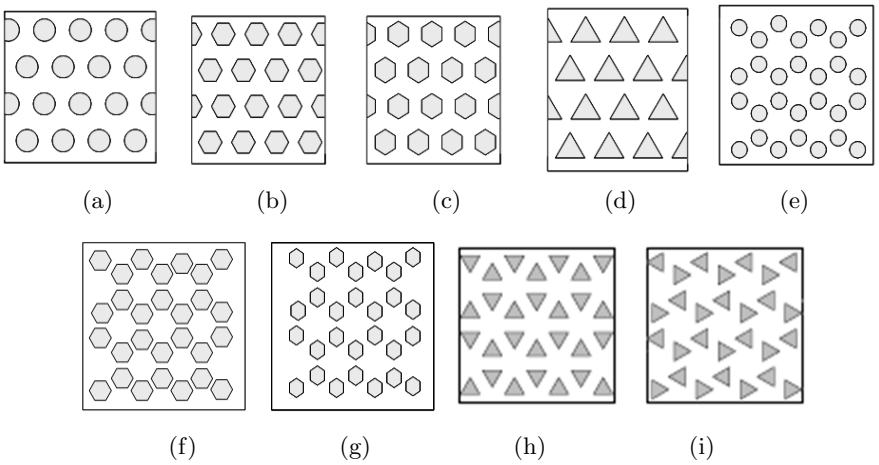

Figure 8. Rod shapes and configurations considered in triangular lattice. (a) triangular-circle (TC). (b) triangular-hexagon (TH). (c) triangular-rotated hexagon (TRH). (d) triangular-triangle (TT). (e) honeycomb-circle (HC). (f) honeycomb-hexagon (HH). (g) honeycomb-rotated hexagon (HRH). (h) honeycomb-triangle (HT). (i) honeycomb-rotated triangle (HRT).

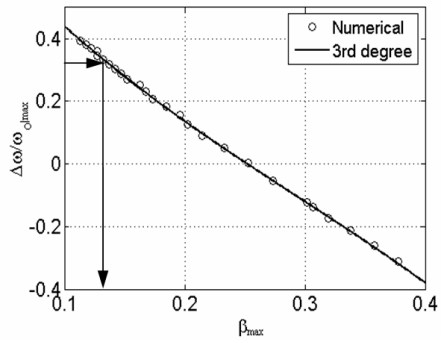

(a) $\Delta\omega/\omega_0|_{\max}$ versus $\beta_{\max}$ for square lattice of circular rods.

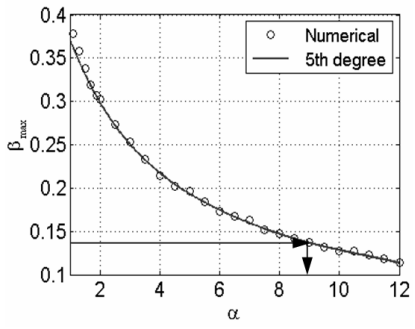

(b) $\beta_{\max}$ versus α for square lattice of circular rods.

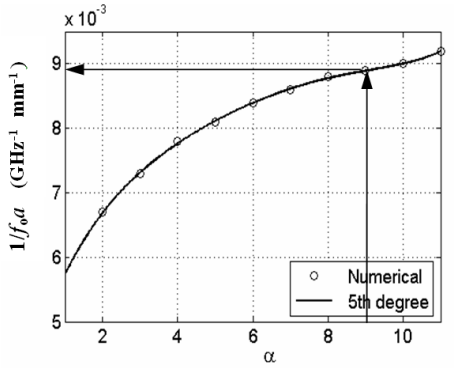

(c) $1/f_0a$ versus α for square lattice of circular rods.

Figure 9. Design steps of a 2-D PBG of square lattice with circular dielectric rods, $f_0 = 6\,\text{GHz}$ and band gap $\Delta f = 2\,\text{GHz}$.

(b) Applying the value of $\beta_{\max}$, it is possible to obtain α by using equation (10a)

For $\beta_{\max} = 0.1333$ the corresponding value of α is found to be 9 as shown in Fig. 9(b)

(c) Finally applying the obtained value of α into the (f_0, α) relation, using equation (12a) where for $\alpha = 9$ we get $1/f_0a = 8.9167 \times 10^{-3}$ as shown in Fig. 9(c)

Thus, the final design parameters at $f_0 = 6\,\text{GHz}$ are found to be $a = 18.7\,\text{mm}$, $r = 3.85\,\text{mm}$, $\varepsilon_a = 9$, and $\varepsilon_b = 1$. Applying these parameters to the PWM simulation program, the resulting band gap is found to be between $f_1 = 5.068\,\text{GHz}$ and $f_2 = 6.99\,\text{GHz}$ as shown

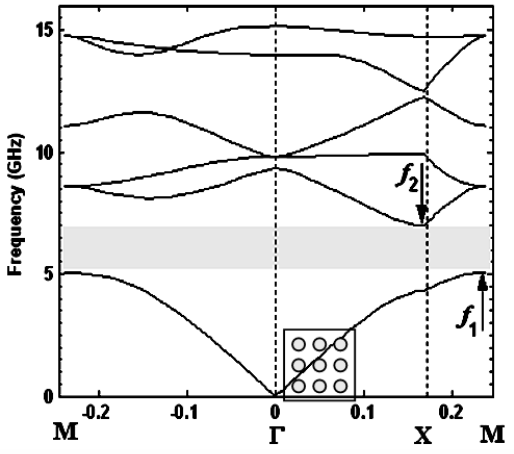

Figure 10. The PWM results of the design example using the parameters obtained from the design equations.

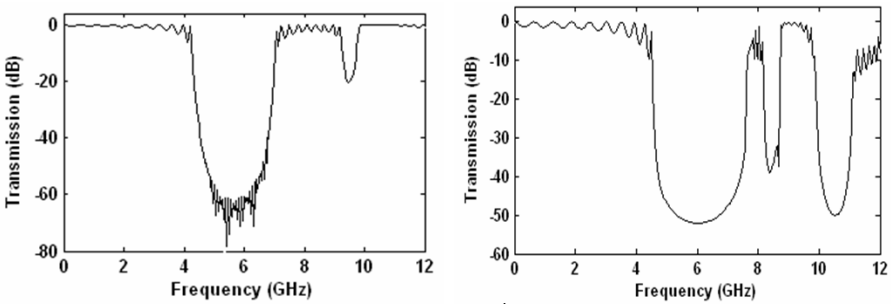

(a) Normal incidence $\theta = 0^\circ,\ \phi = 0^\circ$ (b) Oblique incidence $\theta = 0^\circ,\ \phi = 45^\circ$

Figure 11. Results of FDTD simulation of transmission response for the PBG in Fig. 9.

in Fig. 10. This result shows a good agreement with the pre-required specifications of the design problem.

The transmission response of this PBG structure is also verified by using periodic FDTD algorithm [15]. Ten rods are used to simulate the periodic PBG in the propagation direction, while periodic boundary conditions are applied to simulate infinite periodicities in the other directions. A UPML absorbing boundary condition is used to truncate the domain of analysis in the direction of propagation. A TM_z plane wave Gaussian pulse is used as an excitation for this 2-D periodic

structure by using total field scattered field (TF/SF) formulation [15]. Figure 11 shows the calculated transmission coefficients for this PBG structure for two different angles of incidence. A comparison between the FDTD results and the dispersion diagram of the PWM shows a good agreement where the band gap regions are identical.

5. CONCLUSION

Design formulas for 2D photonic band gap structures are presented. These formulas are obtained by interpolating the results obtained by using plane wave expansion method. The present analysis is applied for both rectangular and triangular lattices that permitted the ability to use different structure forms. The design formulas include the center frequency of operation as a function of the lattice constant, the filling ratio, and the permittivity of host and inclusion. The formulas also include the optimum filling fraction that can be used to obtain maximum bandwidth as a function of the filling ratio, and the maximum bandwidth as a function of the optimum filling fraction.

APPENDIX A.

The previous steps for obtaining design equations are applied on different configurations of PBG structures. These configurations include square and triangular lattice for both TE and TM polarizations and for both $\alpha > 1$ and $\alpha < 1$. The design equations of these structures are summarized in the following tables.

a. Case I ($\alpha > 1$)

For $\alpha > 1$ it is found that the dominant band gap is TM. In this case, it is found that increasing the index ratio causes the peak of the relative bandwidth to take place at a smaller value of the filling fraction.

(1) Square Lattice (TM-Polarization) ($\alpha > 1$)

(2) Triangular Lattice (TM-Polarization) ($\alpha > 1$)

(3) Triangular Honeycomb Lattice (TM-Polarization) ($\alpha > 1$)

In this case, the band gap does not exist between the first two modes as in the previous cases. However, it could be found between the second and the third mode for values of greater than or equal five.

Table A1. Design equations of square lattice PBG structure for TM polarization where ($\alpha > 1$).

Type	No.	Equations
 **SS**	(a)	$\beta_{\max}(\alpha) = -2.3459\times10^{-6}\alpha^5+10.093\times10^{-5}\alpha^4-17.965\times10^{-4}\alpha^3 +17.443\times10^{-3}\alpha^2-0.1037\alpha+0.44203$
	(b)	$\max(\Delta\omega/\omega_0) = 1.7261\beta_{\max}^2 - 3.5588\beta_{\max} + 0.76458$
	(c)	$f_0(a,\alpha) = \dfrac{1/\sqrt{\varepsilon_b}a}{[1.2821\times10^{-7}\alpha^5 - 4.9534\times10^{-6}\alpha^4 + 7.5233\times10^{-5}\alpha^3 -5\ 7535\times10^{-4}\alpha^2+2.4655\times10^{-3}\alpha+3.4394\times10^{-5}]}$
 **SC**	(a)	$\beta_{\max}(\alpha) = -4.141\times10^{-6}\alpha^5+1.6899\times10^{-4}\alpha^4-2.7977\times10^{-3}\alpha^3 +2.4554\times10^{2}\ \hat{a}\ -0.12827\alpha+0.47809$
	(b)	$\max(\Delta\omega/\omega_0) = -8.3658\beta_{\max}^3+7.3676\beta_{\max}^2-4.6609\beta_{\max}+0.84218$
	(c)	$f_0(a,\alpha) = \dfrac{1/\sqrt{\varepsilon_b}a}{[1.5385\times10^{-7}\alpha^5 - 4.9417\times10^{-6}\alpha^4 + 6.3124\times10^{-5}\alpha^3 -4.2991\times10^{-4}\alpha^2+1.8655\times10^{-3}\alpha+4.2527\times10^{-3}]}$
 **SCR**	(a)	$\beta_{\max}(\alpha) = -2.7652\times10^{-6}\alpha^5+1.2653\times10^{-4}\alpha^4-2\ .2657\times10^{-3}\alpha^3 +2.0674\times10^{-2}\alpha^2-0.10866\alpha+0.41462$
	(b)	$\max(\Delta\omega/\omega_0) = -7.6628\beta_{\max}^3+7.1226\beta_{\max}^2-4.9761\beta_{\max}+0.80522$
	(c)	$f_0(a,\alpha) = \dfrac{1/\sqrt{\varepsilon_b}a}{[-2.5641\times10^{-8}\alpha^5 + 5.711\times10^{-7}\alpha^4 - 1.1655\times10^{-8}\alpha^3 -9.6026\times10^{-5}\alpha^2+1.0591\times10^{-3}\alpha+4.7564\times10^{-3}]}$
 **SMCR**	(a)	$\beta_{\max}(\alpha) = -1.5905\times10^{-6}\alpha^5+7.7302\times10^{-5}\alpha^4-1.4995\times10^{-3}\alpha^3 +0.015098\alpha^2-0.089117\alpha+0.38664$
	(b)	$\max(\Delta\omega/\omega_0) = 5.0163\beta_{\max}^3 - 0.3833\beta_{\max}^2 - 3.6507\beta_{\max} + 0.73191$
	(c)	$f_0(a,\alpha) = \dfrac{1/\sqrt{\varepsilon_b}a}{[-5.1282\times10^{-8}\alpha^5+1.6084\times10^{-6}\alpha^4-1.704\times10^{-5}\alpha^3 +4.8392\times10^{-5}\alpha^2+3.7921\times10^{-4}\alpha+0.0037612]}$
 **SRCR**	(a)	$\beta_{\max}(\alpha) = -3.2713\times10^{-6}\alpha^5+1.394\times10^{-4}\alpha^4-0.0023711\alpha^3 +0.020893\alpha^2-0.10728\alpha+0.40572$
	(b)	$\max(\Delta\omega/\omega_0) = -7.8726\beta_{\max}^3+7.6325\beta_{\max}^2-5.2271\beta_{\max}+0.82195$
	(c)	$f_0(a,\alpha) = \dfrac{1/\sqrt{\varepsilon_b}a}{[5.641\times10^{-8}\alpha^5-2.183\times10^{-6}\alpha^4+3.491\times10^{-5}\alpha^3 -0.000301\alpha^2+0.001599\alpha+0.004263]}$
 **SMS**	(a)	$\beta_{\max}(\alpha) = -3.5784\times10^{-6}\alpha^5+1.4982\times10^{-4}\alpha^4-0.0025741\alpha^3 +0.023621\alpha^2-0.12824\alpha+0.48138$
	(b)	$\max(\Delta\omega/\omega_0) = -17.524\beta_{\max}^3+13.646\beta_{\max}^2-5.9793\beta_{\max}+0.91454$
	(c)	$f_0(a,\alpha) = \dfrac{1/\sqrt{\varepsilon_b}a}{[1.9231\times10^{-7}\alpha^5-6.6142\times10^{-6}\alpha^4+8.8258\times10^{-5}\alpha^3 -0.00058429\alpha^2+0.0021297\alpha+0.0021727]}$
 **SRS**	(a)	$\beta_{\max}(\alpha) = -9.8394\times10^{-6}\alpha^5+0.00036373\alpha^4-0.0053214\alpha^3 +0.039907\alpha^2-0.17097\alpha+0.5173$
	(b)	$\max(\Delta\omega/\omega_0) = -9.645\beta_{\max}^3+8.8939\beta_{\max}^2-5.1899\beta_{\max}+0.88357$
	(c)	$f_0(a,\alpha) = \dfrac{1/\sqrt{\varepsilon_b}a}{[1.2626\times10^{-6}\alpha^3-4.9892\times10^{-5}\alpha^2+0.00073131\alpha+0.0055149]}$

Table A2. Design equations of triangular lattice PBG structure for TM polarization where ($\alpha > 1$).

Type	No.	Equations
 **TC**	(a)	$\beta_{\max}(\alpha) = -1.5396\times10^{-5}\alpha^5+5.4826\times10^{-4}\alpha^4-7.6488\times10^{-3}\alpha^3 +5.3722\times10^{-2}\alpha^2-0.21008\alpha+0.55824$
	(b)	$\max(\Delta\omega/\omega_0) = -3.0631\beta_{\max}^3+4.0749\beta_{\max}^2-3.5876\beta_{\max}+0.83159$
	(c)	$f_0(a,\alpha) = \dfrac{1/\sqrt{\varepsilon_b}a}{[1.3908\times10^{-7}\alpha^5-5.024\times10^{-6}\alpha^4+7.0711\times10^{-5}\alpha^3 -4.9953\times10^{-4}\alpha^2+2.0088\times10^{-3}\alpha+3.7983\times10^{-5}]}$
 **TH**	(a)	$\beta_{\max}(\alpha) = -1.5514\times10^{-5}\alpha^5+5.5216\times10^{-4}\alpha^4-7.6984\times10^{-3}\alpha^3 +5.4011\times10^{-2}\alpha^2-0.21072\alpha+0.55806$
	(b)	$\max(\Delta\omega/\omega_0) = -2.9776\beta_{\max}^3+4.0585\beta_{\max}^2-3.5973\beta_{\max}+0.83178$
	(c)	$f_0(a,\alpha) = \dfrac{1/\sqrt{\varepsilon_b}a}{[8.1453\times10^{-8}\alpha^5-3.2708\times10^{-6}\alpha^4+5.1599\times10^{-5}\alpha^3 -4.0964\times10^{-4}\alpha^2+1.8313\times10^{-3}\alpha+3.9154\times10^{-3}]}$
 **TRH**	(a)	$\beta_{\max}(\alpha) = 2.3817\times10^{-5}\alpha^4-0.00082916\alpha^3+0.011697\alpha^2 -0.08932\alpha+0.43282$
	(b)	$\max(\Delta\omega/\omega_0) = -16.818\beta_{\max}^3+10.823\beta_{\max}^2-4.5364\beta_{\max}+0.86926$
	(c)	$f_0(a,\alpha) = \dfrac{1/\sqrt{\varepsilon_b}a}{[2\times10^{-6}\alpha^3-6.7\times10^{-5}\alpha^2-0.00083\alpha+0.0048]}$
 **TT**	(a)	$\beta_{\max}(\alpha) = -1.8745\times10^{-5}\alpha^5+6.5795\times10^{-4}\alpha^4-8.984\times10^{-3}\alpha^3 +6.0953\times10^{-2}\alpha^2-0.22452\alpha+0.54599$
	(b)	$\max(\Delta\omega/\omega_0) = -1.8663\beta_{\max}^3+4.3259\beta_{\max}^2-3.8945\beta_{\max}+0.81259$
	(c)	$f_0(a,\alpha) = \dfrac{1/\sqrt{\varepsilon_b}a}{[-1.1281\times10^{-8}\alpha^5-1.5326\times10^{-7}\alpha^4+1.1936\times10^{-5}\alpha^3 -1.7355\times10^{-4}\alpha^2+1.1824\times10^{-3}\alpha+4.465\times10^{-3}]}$

Table A3. Design equations of triangular lattice-Honeycomb PBG structures for TM polarization where ($\alpha > 1$).

Type	No.	Equations
 **HC$_{23}$**	(a)	$\beta_{\max}(\alpha) = -1.465 \times 10^{-5}\alpha^5 + 0.00051881\alpha^4 - 0.0071957\alpha^3 + 0.050304\alpha^2 - 0.19811\alpha + 0.57617$
	(b)	$\max(\Delta\omega/\omega_0) = -0.40627\beta^3_{\max} + 1.5514\beta^2_{\max} - 3.6206\beta_{\max} + 0.75432$
	(c)	$f_0(a,\alpha) = \dfrac{1/\sqrt{\varepsilon_b}a}{[5.5621\times10^{-8}\alpha^5 - 2.2606\times10^{-6}\alpha^4 + 3.6281\times10^{-5}\alpha^3 - 0.00029768\alpha^2 + 0.0014396\alpha + 0.0025359]}$
 **HH$_{23}$**	(a)	$\beta_{\max}(\alpha) = -1.4316 \times 10^{-5}\alpha^5 + 0.00050848\alpha^4 - 0.0070766\alpha^3 + 0.049659\alpha^2 - 0.19636\alpha + 0.57352$
	(b)	$\max(\Delta\omega/\omega_0) = -0.41023\beta^3_{\max} + 1.5809\beta^2_{\max} - 3.6425\beta_{\max} + 0.75503$
	(c)	$f_0(a,\alpha) = \dfrac{1/\sqrt{\varepsilon_b}a}{[5.5621\times10^{-8}\alpha^5 - 2.2606\times10^{-6}\alpha^4 + 3.6281\times10^{-5}\alpha^3 - 0.00029768\times\alpha^2 + 0.0014396\alpha + 0.0025359]}$
 **HRH$_{23}$**	(a)	$\beta_{\max}(\alpha) = -4.2291 \times 10^{-6}\alpha^5 + 0.0001988\alpha^4 - 0.0036243\alpha^3 + 0.032746\alpha^2 - 0.16156\alpha + 0.55062$
	(b)	$\max(\Delta\omega/\omega_0) = 1.4076\beta^2_{\max} - 3.6361\beta_{\max} + 0.75771$
	(c)	$f_0(a,\alpha) = \dfrac{1/\sqrt{\varepsilon_b}a}{[5.5621\times10^{-8}\alpha^5 - 2.2606\times10^{-6}\alpha^4 + 3.6281\times10^{-5}\alpha^3 - 0.00029768\alpha^2 + 0.0014396\alpha + 0.0025359]}$
 **HRT$_{23}$**	(a)	$\beta_{\max}(\alpha) = -1.8399 \times 10^{-5}\alpha^5 + 0.00064739\alpha^4 - 0.0088564\alpha^3 + 0.060168\alpha^2 - 0.22312\alpha + 0.58141$
	(b)	$\max(\Delta\omega/\omega_0) = 2.1853\beta^3_{\max} + 0.87509\beta^2_{\max} - 3.762\beta_{\max} + 0.72024$
	(c)	$f_0(a,\alpha) = \dfrac{1/\sqrt{\varepsilon_b}a}{[2.3331\times10^{-8}\alpha^5 - 1.2991\times10^{-6}\alpha^4 + 2.5889\times10^{-5}\alpha^3 - 0.00024715\alpha^2 + 0.0013192\alpha + 0.0025987]}$
 **HT$_{23}$**	(a)	$\beta_{\max}(\underset{2}{\alpha}) = -1.2913 \times 10^{-5}\alpha^5 + 0.0004595\alpha^4 - 0.0064113\alpha^3 + 0.045119\alpha - 0.17823\alpha + 0.51686$
	(b)	$\max(\Delta\omega/\omega_0) = -4.2198\beta^3_{\max} + 5.7629\beta^2_{\max} - 5.0873\beta_{\max} + 0.79864$
	(c)	$f_0(a,\alpha) = \dfrac{1/\sqrt{\varepsilon_b}a}{[5.635\times10^{-9}\alpha^5 - 6.8744\times10^{-7}\alpha^4 + 1.7868\times10^{-5}\alpha^3 - 0.00019791\alpha^2 + 0.0011802\alpha + 0.0027391]}$

b. Case II ($\alpha < 1$)

For the case of $\alpha < 1$, the dominant band gap is found to be of TE polarization. In this case, decreasing the index ratio causes the peak of the relative bandwidth to take place at a larger value of the filling fraction.

(1) Square Lattice (TE-Polarization) ($\alpha < 1$)

(2) Triangular Lattice (TE-Polarization) ($\alpha < 1$)

(3) Triangular Lattice-Honeycomb Structures (TE-Polarization) where $\alpha < 1$)

In this case, the first band gap exists between the 3rd and 4th mode of the structure of $\alpha \leq 1/4$.

Table A4. Design equations of square lattice PBG structure for TE polarization where ($\alpha < 1$).

Type	No.	Equations
 SS	(a)	$\beta_{\max}(\alpha) = 17.761\alpha^4 - 23.538\alpha^3 + 11.656\alpha^2 - 2.9292\alpha + 0.839$
	(b)	$\max(\Delta\omega/\omega_0) = 2.4119\beta_{\max} - 1.3341$
	(c)	$f_0(a,\alpha) = \dfrac{1/\sqrt{\varepsilon_a}a}{3.0418\times10^{-6}\alpha^{-3} - 8.9561\times10^{-5}\alpha^{-2} + 1.0218\times10^{-3}\alpha^{-1} + 5.0011\times10^{-3}}$
 SC	(a)	$\beta_{\max}(\alpha) = 0.34147\alpha^2 - 0.53021\alpha + 0.59739$
	(b)	$\max(\Delta\omega/\omega_0) = 2.7544\beta_{\max}^2 - 0.3744\beta_{\max} - 0.54748$
	(c)	$f_0(a,\alpha) = \dfrac{1/\sqrt{\varepsilon_a}a}{3.0923\times10^{-6}\alpha^{-3} - 7.9818\times10^{-5}\alpha^{-2} + 1.0737\times10^{-3}\alpha^{-1} + 4.94\times10^{-3}}$
 SRCR	(a)	$\beta_{\max}(\alpha) = 0.51095\alpha^2 - 0.54786\alpha + 0.51162$
	(b)	$\max(\Delta\omega/\omega_0) = 3.3459\beta_{\max} - 1.4782$
	(c)	$f_0(a,\alpha) = \dfrac{1/\sqrt{\varepsilon_a}a}{-3.3098\times10^{-5}\alpha^{-2} + 0.00088589\alpha^{-1} + 0.0053759}$
 SMS	(a)	$\beta_{\max}(\alpha) = 0.45116\alpha^2 - 0.62026\alpha + 0.59677$
	(b)	$\max(\Delta\omega/\omega_0) = 2.0839\beta_{\max} - 1.0705$
	(c)	$f_0(a,\alpha) = \dfrac{1/\sqrt{\varepsilon_a}a}{-1.7439\times10^{-5}\alpha^{-2} + 0.00054032\alpha^{-1} + 0.0038746}$

Table A5. Design equations of triangular lattice PBG structure for TE polarization where ($\alpha < 1$).

Type	No.	Equations
 **TC**	(a)	$\beta_{\max}(\alpha) = 0.89764\alpha^2 - 0.92777\alpha + 0.72132$
	(b)	$\max(\Delta\omega/\omega_0) = 2.7806\beta_{\max} - 1.3252$
	(c)	$f_0(a,\alpha) = \dfrac{1/\sqrt{\varepsilon_a}a}{3.3411\times10^{-6}\alpha^{-3} - 9.1667\times10^{-5}\alpha^{-2} + 1.0004\times10^{-3}\alpha^{-1} + 4.8712\times10^{-3}}$
 **TH**	(a)	$\beta_{\max}(\alpha) = 0.17\alpha^2 - 0.196\alpha + 0.1978$
	(b)	$\max(\Delta\omega/\omega_0) = 10.7\beta_{\max} - 1.52$
	(c)	$f_0(a,\alpha) = \dfrac{1/\sqrt{\varepsilon_a}a}{2.7972\times10^{-6}\alpha^{-3} - 7.8788\times10^{-5}\alpha^{-2} + 9.7902\times10^{-4}\alpha^{-1} + 4.857\times10^{-3}}$
 **TRH**	(a)	$\beta_{\max}(\alpha) = 0.90426\alpha^2 - 0.93421\alpha + 0.72425$
	(b)	$\max(\Delta\omega/\omega_0) = 2.8723\beta_{\max} - 1.3779$
	(c)	$f_0(a,\alpha) = \dfrac{1/\sqrt{\varepsilon_a}a}{3.2822\times10^{-6}\alpha^{-3} - 9.2682\times10^{-5}\alpha^{-2} + 0.0010145\times\alpha^{-1} + 0.0048288}$

Table A6. Design equations of triangular lattice-Honeycomb PBG structures for TE polarization where ($\alpha < 1$).

Type	No.	Equations
 **HC_{34}**	(a)	$\beta_{\max}(\alpha) = 5.0351\alpha^5 - 7.9194\alpha^4 + 5.5546\alpha^3 - 2.1886\alpha^2 + 0.27525\alpha + 0.32336$
	(b)	$\max(\Delta\omega/\omega_0) = 25.819\beta_{\max}^2 - 13.398\beta_{\max} + 1.6684$
	(c)	$f_o(a,\alpha) = \dfrac{1/\sqrt{\varepsilon_a}a}{1.6667\times10^{-5}\alpha^{-2} + 0.00064636\alpha^{-1} + 0.0027903}$
 **HH_{34}**	(a)	$\beta_{\max}(\alpha) = -9.7316\alpha^5 + 10.683\alpha^4 - 2.9166\alpha^3 - 0.47732\alpha^2 + 0.12346\alpha + 0.32751$
	(b)	$\max(\Delta\omega/\omega_0) = 25.359\beta_{\max}^2 - 13.104\beta_{\max} + 1.6227$
	(c)	$f_o(a,\alpha) = \dfrac{1/\sqrt{\varepsilon_a}a}{1.6667\times10^{-5}\alpha^{-2} + 0.00064636\alpha^{-1} + 0.0027903}$
 **HRH_{34}**	(a)	$\beta_{\max}(\alpha) = 6.0933\alpha^5 - 9.3461\alpha^4 + 6.0797\alpha^3 - 2.1752\alpha^2 + 0.25944\alpha + 0.31445$
	(b)	$\max(\Delta\omega/\omega_0) = 31.487\beta_{\max}^2 - 16.189\beta_{\max} + 2.0106$
	(c)	$f_o(a,\alpha) = \dfrac{1/\sqrt{\varepsilon_a}a}{1.5152\times10^{-5}\alpha^{-2} + 0.00063212\alpha^{-1} + 0.0028364}$
 **HRT_{34}**	(a)	$\beta_{\max}(\alpha) = 0.24887\alpha^2 - 0.35064\alpha + 0.34058$
	(b)	$\max(\Delta\omega/\omega_0) = 1.6796\beta_{\max} - 0.46598$
	(c)	$f_o(a,\alpha) = \dfrac{1/\sqrt{\varepsilon_a}a}{2.0837\times10^{-6}\alpha^{-3} - 5.9477\times10^{-5}\alpha^{-2} + 0.00088895\alpha^{-1} + 0.0025099}$
 **HT_{34}**	(a)	$\beta_{\max}(\alpha) = 21.019\alpha^4 - 24.323\alpha^3 + 10.828\alpha^2 - 2.4772\alpha + 0.57519$
	(b)	$\max(\Delta\omega/\omega_0) = -17.239\alpha^3 + 16.959\alpha^2 - 3.8933\alpha + 0.078782$
	(c)	$f_o(a,\alpha) = \dfrac{1/\sqrt{\varepsilon_a}a}{3.7296\times10^{-6}\alpha^{-3} - 10.0\times10^{-5}\alpha^{-2} + 0.0010841\alpha^{-1} + 0.0021188}$

REFERENCES

1. Guida, G., A. de Lustrac, and A. Priou, "An introduction to photonic band gap (PBG) materials," *Progress In Electromagnetics Research*, PIER 41, 1–20, 2003.
2. Lee, R. K., Y. Xu, and A. Yariv, "Microcavities photonic bandgaps and applications to lasers and optical communications," *IEEE Lasers and Electro-Optics Society 1999 12th Annual Meeting. LEOS '99*, 1999.
3. Bayindir, M. and E. Ozbay, "Band-dropping via coupled photonic crystal waveguides," *Optics Express*, Vol. 10, No. 22, 1279–1284, Nov. 2002.
4. Cuesta-Soto, F., A. Martnez, J. Garca, F. Ramos, P. Sanchis, J. Blasco, and J. Mart, "All-optical switching structure based on a photonic crystal directional coupler," *Optics Express*, Vol. 12, No. 1, 161–167, Jan. 2004.
5. Chen, C., S. Shi, D. W. Prather, and A. Sharkawy, "Beam steering with photonic crystal horn radiators," *Optical Engineering*, Vol. 43, No. 1, 174–180, Jan. 2004.
6. Chien, F. S., Y. J. Hsu, W. F. Hsieh, and S. C. Cheng, "Dual wavelength demultiplexing by coupling and decoupling of photonic crystal waveguides," *Optics Express*, Vol. 12, No. 6, 1119–1125, Mar. 2004.
7. Ozbay, E., B. Temelkuran, and M. Bayindir, "Microwave applications of photonic crystals," *Progress In Electromagnetics Research*, PIER 41, 185–209, 2003.
8. Rahmat-Samii, Y. and H. Mosallaei, "Electromagnetic bandgap structures: classification, characterization, and applications," *International Conference on Antennas and Propagation*, 17–20, Manchester, Apr. 2001.
9. Pottier, P., C. Seassal, X. Letartre, J. L. Leclercq, P. Viktorovitch, D. Cassagne, and C. Jouanin, "Triangular and hexagonal high Q-factor 2-D photonic bandgap cavities on III-V suspended membranes," *Journal of Lightwave Technology*, Vol. 17, No. 11, 2058–2062, Nov. 1999.
10. Smirnova, E. I., C. Chen, M. A. Shapiro, and R. J. Temkin, "Simulation of metallic photonic bandgap structures for accelerator applications," *IEEE Particle Accelerator Conference, 2001, PAC*, 933–935, 2001.
11. Smirnova, E. I., C. Chen, M. A. Shapiro, J. R. Sirigiri, and R. J. Temkin, "Simulation of photonic band gaps in metal rod lattices for microwave applications," *Journal of Applied Physics*,

Vol. 91, No. 3, 960–968, Feb. 2002.

12. Chen, M. Y. and R. J. Yu, "Analysis of photonic bandgaps in modified honeycomb structures," *IEEE Photonics Technology Letters*, Vol. 16, No. 3, 819–821, Mar. 2004.
13. Silveirinha, M. G. and C. A. Fernandes, "A hybrid method for the efficient calculation of the band structure of 3-D metallic crystals," *IEEE Transactions on Microwave Theory and Techniques*, Vol. 52, No. 3, 889–902, Mar. 2004.
14. Ward, A. J., "Transfer matrices, photonic bands and related quantities," *Imperial College of Science, Technology and Medicine*, London, July 1996.
15. Taflove, A. and S. C. Hagness, *Computational Electrodynamics: the Finite-Difference Time-Domain Method*, 2nd edition, Artech House, Norwood, MA, 2000.
16. Pelosi, G., R. Coccioli, and S. Selleri, *Quick Finite Element Method for Electromagnetic Waves*, Chapter 5, Artech House, 1998.
17. Zheng, L. G. and W. X. Zhang, "Study on bandwidth of 2-D dielectric PBG material," *Progress In Electromagnetics Research*, PIER 41, 83–106, 2003.
18. Brillouin, L., *Wave Propagation in Periodic Structures*, Chapter VI, Dover Publications, Inc., 1946.
19. Luan, P. and Z. Ye, "Two dimensional photonic crystals," available on line at http://arxiv.org/PS_cache/cond-mat/pdf/0105/0105428v1.pdf